Multiple genetic pathways regulating lifespan extension are neuroprotective in a G2019S LRRK2 nematode model of Parkinson's disease

Megan M. Senchuk[a], **Jeremy M. Van Raamsdonk**[b,c,d,**], **Darren J. Moore**[a,*]

[a]Department of Neurodegenerative Science, Van Andel Institute, Grand Rapids, MI 49503, USA

[b]Department of Neurology and Neurosurgery, McGill University, Montreal, Quebec H4A 3J1, Canada

[c]Metabolic Disorders and Complications Program, Brain Repair and Integrative Neuroscience Program, Research Institute of the McGill University Health Centre, Montreal, Quebec H4A 3J1, Canada

[d]Department of Genetics, Harvard Medical School, Cambridge, MA 02115, USA

Abstract

Mutations in the *leucine-rich repeat kinase 2* (*LRRK2*) gene are the most frequent cause of late-onset, familial Parkinson's disease (PD), and *LRRK2* variants are associated with increased risk for sporadic PD. While advanced age represents the strongest risk factor for disease development, it remains unclear how different age-related pathways interact to regulate *LRRK2*-driven late-onset PD. In this study, we employ a *C. elegans* model expressing PD-linked G2019S LRRK2 to examine the interplay between age-related pathways and LRRK2-induced dopaminergic neurodegeneration. We find that multiple genetic pathways that regulate lifespan extension can provide robust neuroprotection against mutant LRRK2. However, the level of neuroprotection does not strictly correlate with the magnitude of lifespan extension, suggesting that lifespan can be experimentally dissociated from neuroprotection. Using tissue-specific RNAi, we demonstrate that lifespan-regulating pathways, including insulin/insulin-like growth factor-1 (IGF-1) signaling, target of rapamycin (TOR), and mitochondrial respiration, can be directly manipulated in neurons to mediate neuroprotection. We extend this finding for AGE-1/PI3K, where pan-neuronal versus dopaminergic neuronal restoration of AGE-1 reveals both cell-autonomous and non-cell-autonomous neuroprotective mechanisms downstream of insulin signaling. Our data demonstrate the importance of distinct lifespan-regulating pathways in the pathogenesis of *LRRK2*-linked PD, and suggest that extended longevity is broadly neuroprotective via the actions of these pathways at least in part within neurons. This study further highlights the complex interplay that occurs between cells and tissues during organismal aging and disease manifestation.

1. Introduction

Parkinson's disease (PD) is a common neurodegenerative disorder, affecting 1–2% of individuals over 65 years of age (de Lau and Breteler 2006). With population demographics predicting an increasingly elderly population, the prevalence of PD is expected to grow to over 12 million cases by 2040 (Collaborators 2019; Dorsey et al. 2018). PD is a progressive movement disorder characterized by resting tremor, muscular rigidity, and bradykinesia primarily resulting from the selective degeneration of dopaminergic neurons in the substantia nigra and the corresponding loss of nigrostriatal pathway dopamine signaling. While PD is influenced by both genetic risk and environmental exposure, the etiology of PD remains unclear. Aging is considered a primary risk factor for the development of PD, as the incidence of disease rises exponentially with increasing age (Billingsley et al. 2018). Aging is associated with the impairment of numerous cellular pathways, including mitochondrial respiration, proteostasis, autophagy and stress responses that lead to a reduced chaperone response and increased genomic instability. A number of pathways have been identified that can regulate chronological age yet the relationship between these specific lifespan-regulating pathways and pathogenic mechanisms underlying PD are poorly understood.

The identification of genetic mutations linked to familial forms of PD have provided important insight into disease pathophysiology. Mutations in *leucine-rich repeat kinase 2* (*LRRK2*) cause late-onset, autosomal dominant familial PD that is largely indistinguishable from sporadic disease, whereas both coding and non-coding variants are associated with an increased risk of sporadic PD (Hernandez et al. 2016). *LRRK2* encodes a multidomain protein containing kinase, GTPase, and protein-protein interaction domains, with familial mutations commonly leading to enhanced kinase activity (Steger et al. 2016; West et al. 2005). The biological functions of LRRK2 remain to be fully elucidated, although prior studies suggest roles in diverse cellular processes, including vesicular transport/sorting, endocytosis, autophagy, mitochondrial dynamics, and lysosomal function (Erb and Moore 2020). Familial LRRK2 mutations share the capacity to induce neuronal damage in culture models via a kinase-dependent mechanism (Islam and Moore 2017), whereas increased LRRK2 kinase activity has been reported in PD-linked *D620N VPS35* knockin mice and sporadic PD brain (Di Maio et al. 2018; Mir et al. 2018). LRRK2 kinase activation may therefore represent a common mechanism underlying PD pathogenesis (Kluss et al. 2019), and a promising target for therapeutic disease-modification.

Among familial *LRRK2* mutations, G2019S is the most common, accounting for 5–6% of familial PD and 1–2% of sporadic PD in the US population (Billingsley et al. 2018). PD linked to the G2019S mutation is typically late-onset and exhibits variable yet age-dependent penetrance depending on ethnicity, with estimates of cumulative risk rising from ~20% at 50 years to ~75% at 80 years of age (Spatola and Wider 2014). The exponential rise

in PD risk after age 50 suggests that the aging process may play an important role in manifesting the pathogenic actions of *LRRK2* mutations (Marder et al. 2015). This interaction of age with LRRK2 is borne out in experimental models, such as G2019S LRRK2 knockin or transgenic mice, *Drosophila* or *C. elegans*, that develop age-dependent and often late-onset PD-like phenotypes (Ho et al. 2020; Longo et al. 2017; Ramonet et al. 2011; Xiong et al. 2018; Yao et al. 2010). Some individuals harboring *LRRK2* mutations escape PD within their lifetime, suggesting that genetic variation within different age-related pathways might feasibly be protective and could be manipulated to prevent disease.

While incomplete penetrance suggests that age-related pathways significantly interact with G2019S LRRK2 during disease progression, experimental mammalian models including human induced pluripotent stem cells and rodent models are cost-prohibitive or not practical for chronic aging studies. We therefore took advantage of the nematode *Caenorhabditis elegans*, a well-established model for aging studies, to systematically investigate functional interactions between age-related pathways and G2019S LRRK2-induced dopaminergic neurodegeneration. Conserved signaling pathways regulating the aging process include insulin/insulin-like growth factor-1 (IGF-1) signaling, target of rapamycin (TOR) pathway, the 5′ AMP-activated protein kinase (AMPK) cascade, signals from the reproductive system, environmental sensing, and caloric restriction. These pathways define major nutrient-sensing, endocrine, and stress response signaling pathways, and are required for the coordinated regulation of systemic organismal aging.

Our recent study demonstrated that reducing insulin/IGF-1 signaling via *daf-2* disruption, a well-characterized pathway for regulating lifespan, increased dopaminergic viability in *C. elegans* models of PD expressing human mutant LRRK2 or α-synuclein (Cooper et al. 2015). However, the underlying mechanism for this neuroprotective effect is not clear. It is possible that insulin/IGF-1 signaling interacts directly with G2019S LRRK2 to attenuate neurodegenerative phenotypes, and would therefore represent a potential therapeutic pathway. Alternatively, reduced insulin signaling may act indirectly by slowing the rate of aging in all tissues, and this feature may regulate LRRK2-induced neurotoxicity. To distinguish between lifespan extension in general versus the insulin signaling pathway as a key neuroprotective mechanism, we evaluate and compare the neuroprotective effects of multiple distinct lifespan-extending pathways in the G2019S LRRK2 worm model. Our data demonstrate that lifespan extension via multiple signaling pathways can regulate dopaminergic neuronal resilience toward G2019S LRRK2.

2. Methods

2.1. C. elegans strains and maintenance

Unless noted, strains were maintained at 20 °C on NGM seeded with OP50 bacteria according to standard practice (Brenner 1974). Transgenic cwrIs856 [Pdat-1::GFP, Pdat-1::LRRK2(G2019S), lin-15(+)] has been previously described (Cooper et al. 2015; Yao et al. 2010). Double mutants were constructed as detailed elsewhere (Cooper et al. 2015). *daf-2* animals were raised at 15 °C and shifted to 20 °C at L4 stage. *glp-1* animals were raised at 15 °C and shifted to 25 °C as embryos to obtain germline (−/−) adults. cwrIs856 [pDat-1::GFP; pDat-1::LRRK2 (G2019S)] were treated similarly in all conditions to serve as

controls. For all assays, a minimum of three biological replicates (~40 worms) per strain were assayed. All assays were performed by an experimenter blinded to genotype.

2.2. Lifespan analysis

Worm populations were synchronized by washing a well-seeded plate to remove adults and larvae, leaving a population of embryos. After 2–3 days, upon reaching young adulthood, 30–40 worms were transferred to NGM plates containing 25 μM fluorodeoxyuridine (FUdR); inclusion of this DNA synthesis inhibitor prevents hatching of progeny following the initial transfer (at 48 h post-plating). FUdR has minimal effects on longevity at this concentration (Van Raamsdonk and Hekimi 2011), and does not affect expression levels or localization of GFP transgenes. Animals were transferred to fresh plates weekly, and viability was scored every 2 days by gentle prodding with a platinum pick. Animals that failed to respond were scored as dead. Worms that died from internal hatching of progeny, expulsion of internal contents or desiccation on the side of the dish were censored and excluded from analysis (refer to Tables S1–S8 for animal numbers used). Mutation and RNAi conditions increase number of censored worms.

2.3. Dopaminergic neuronal damage

Dopaminergic neurons were marked by GFP expression driven by the dopamine transporter (DAT-1) promoter. To quantify damage and compare across treatments, we developed a scoring metric of 0–5, with a score of 0 given to healthy, unbroken, bright, thick axons and cell bodies lacking punctate structures, as these are not observed in pDat-1::GFP-expressing strains that lack the LRRK2(G2019S) transgene. A score of 5 was given to neurons severely damaged (multiple puncta and/or cell body morphology defects) or undetectable GFP. Transmission electron microscopy has been used previously to demonstrate that loss of GFP in these neurons correlates with ultrastructural damage consistent with apoptotic cell death by (Nass et al. 2002).

Quantitative analyses of dopaminergic degeneration was performed by immobilizing 20–40 worms (unless stated otherwise, aged to Day 14 on 25 μM FUdR) on a 1.5% agarose pad with 5 mM levamisole. Live worms on coverslipped slides were immediately scored at 40× using a Leica upright epifluorescent microscope (DM5500 B). Unless noted otherwise, all images are maximum projection composite micrographs collected on a Nikon A1plus-RSi scanning confocal microscope. Images were collected every 0.5 μm over 30 μm, capturing the cell body and axonal projections of pDat-1::GFP-labeled cephalic sensilla (CEP) neurons. All images shown are representative of multiple independent experiments. Refer to Tables S1–S8 for animal numbers used in each experiment.

2.4. RNAi

Standard NGM agar was supplemented with 50 μg/ml carbenicillin and 5 mM isopropyl β-D-1-thiogalactopyranoside (IPTG) post-autoclaving and allowed to dry overnight at room temperature. RNAi cultures were prepared by sequence verifying single colony cultures from the Ahringer RNAi plasmid library. *E. coli* HT115 carrying sequence-verified RNAi targeting plasmid clones were grown in LB supplemented with 50 μg/ml carbenicillin and grown for 8 h at 37 °C. Cultures were concentrated 5× prior to seeding plates with 200 μl of

RNAi bacteria, which was spread, dried, and allowed to induce dsRNA expression for 48 h at RT, after which point plates were stored at 4 °C for up to 1 week. HT115 carrying the pL4440 plasmid lacking a gene-targeting cassette was used as a control for all RNAi experiments (empty vector).

RNAi knockdown was initiated by plating L4 P_O animals to prepared plates. After 30–35 h, adult animals were transferred to fresh RNAi plates and allowed to lay for 12 h, after which point adults were removed. After an additional ~50 h, when embryos laid on RNAi plates had developed to young adulthood, animals were transferred to fresh RNAi plates containing 25 μM (FUdR) in addition to carbenicillin and IPTG.

Neuron-specific RNAi was performed by crossing TU3401 (*sid-1* (pk3321); uIs69[pCFJ90(myo-2p::mCherry) + unc-119p::sid-1]) (Calixto et al. 2010) to cwrIs856 [pDat-1::GFP; pDat-1::LRRK2(G2019S)]. Lifespan and neuronal damage were assayed as above, however, due to the modestly shortened lifespan attributed to *sid-1*(pk3321) in the periphery, dopaminergic neuronal damage was assayed at Day 11, a point at which control animals show equivalent damage to non-*sid-1* animals at Day 14.

2.5. Construction of AGE-1 transgenics

Tissue-specific rescue transgenic expression constructs of the AGE-1 ORF were generated by standard Multi-site Gateway cloning methods. Full-length *age-1* cDNA was PCR-amplified using Phusion High-Fidelity DNA Polymerase+GC buffer (Thermofisher) using total cDNA prepared from N2 mRNA (Ampliscribe). AttB1 and AttB2 adaptors were added to the 5′ end of the forward and reverse primers, respectively, to allow for BP-mediated recombination into a pDONR221 vector (Invitrogen). The resulting entry clone was sequence verified. LR recombination (Invitrogen) was used to generate AGE-1 flanked by a 5′ promoter element (either pan-neuronal pUnc-119 or dopaminergic-specific pDat-1, both from Dharmacon), and a 3′UTR (pADA-126; let-858 3′UTR in pDONRP2R-P3) in the pCFJ150 MosSCI destination vector. Resulting expression plasmids were confirmed by diagnostic digest. Injection mixes were prepared by digesting pMS16 (pUnc-119::AGE-1::let-858) and pMS17 (pDat-1::AGE-1::let-858) with *Age*I and Srf1; the resulting ~11.6 kb band was gel purified and injected into N2 animals at 5 ng/μl with co-marker (pMyo-3::RFP (bsem1122) at 5 ng) and carrier DNA (sheared salmon testis DNA) to 100 ng/μl. The presence of the AGE-1 ORF transgene was verified in RFP-positive lines by PCR. AGE-1/RFP double-positive arrays were then crossed to *age-1*(hx546); cwrIs856 [pDat-1::GFP; pDat-1::LRRK2(G2019S)] to generate tissue-specific restoration lines. Homozygosity of the *hx546* missense mutant was confirmed using intron-specific primers, allowing for genomic locus-specific sequencing.

2.6. Quantitative RT-PCR

Worms were synchronized by washing for laid embryos, which were then allowed to hatch and were raised on OP50 until the L4 stage, at which point worms were transferred to 25 μM FUdR plates seeded with OP50 (Day 1). Populations were washed to fresh plates ever 2–3 days to remove dead embryos and maintain bacterial food supply. At days 5 and 10, worm populations were washed 3 times in M9, collected by settling, and the worm pellet was flash

frozen in liquid nitrogen. Total RNA was extracted using Trizol reagent by standard methods and DNase-digested to remove genomic DNA. cDNA was transcribed from 1 μg of total RNA using a High Capacity cDNA Reverse Transcription Kit (Life Technologies) according to the manufacturer's protocol. Samples processed similarly but lacking the reverse transcriptase enzyme served as a negative control and were subtracted from Ct values as copy number. qPCR was set up using 1 μl of cDNA and FastStart Universal SYBR Green kit (Roche). Human LRRK2 or GFP mRNA expression levels from at least three biological replicates collected on different days were normalized to the levels of *act-3*. The following primer pairs were used for qPCR: act-3-RT-FOR, 5′-GCCCAATCCAAGAGAGGTAA-3′ and act-3-RT-REV, 5′-GGCTTCAGTGAGGAGGACTG-3′; LRRK2-RT-FOR, 5′-CCCTGTGATTCTCGTTGGCAC-3′ and LRRK2-RT-REV, 5′-GCAGGGAACCCTCGCTTATTC-3′; mEGFP-RT-FOR, 5′-CACATGAAGCAGCACGAC-3′ and mEGFP-RT-REV, 5′-CGAACTTCACCTCGGCG-3′.

2.7. Statistical analysis

All statistical analyses were conducted using GraphPad Prism. Life-span assays were assessed using the log-rank test to compare survival curves. Statistical significance of differences of lifespan means and dopaminergic neuronal damage was determined using a one-way ANOVA with Dunnett's post-hoc test to identify specific differences. Data are presented as mean ± standard error of the mean (SEM).

2.8. C. elegans strains used in this study

Strain	Genotype	Original publication
DJM003	cwrIs856 [Pdat-1::GFP, Pdat-1::LRRK2 (G2019S), lin-15(+)]	(Yao et al. 2010)
SGC851	cwrIs851 [Pdat-1::GFP, (Pdat-1::LRRK2 (R1441C), lin-15(+)]	(Yao et al. 2010)
SGC730	cwrIs730 [Pdat-1::GFP, lin-15(+)]	(Yao et al. 2010)
SGC722	cwrIs722 [Pdat-1::GFP, Pdat-1::LRRK2 (WT), lin-15(+)]	(Yao et al. 2010)
CB1370	daf-2(e1370) III	(Kenyon et al. 1993; Kimura et al. 1997)
TJ1052	age-1(hx546) II	(Friedman and Johnson 1988)
MQ1333	nuo-6(qm200) I	(Yang and Hekimi 2010)
CB4037	glp-1(e2141) III	(Arantes-Oliveira et al. 2002; Priess et al. 1987)
DA1116	eat-2(ad1116) II	(Lakowski and Hekimi 1998)
KX15	ife-2(ok306) X	(Syntichaki et al. 2007)
VC265	osm-5(ok451) X	(Apfeld and Kenyon 1999)
RB1206	rsks-1(ok1255) III	(Hansen et al. 2007; Pan et al. 2007)
JVR202	daf-2(e1370) III; cwrIs856 [Pdat-1::GFP, Pdat-1::LRRK2(G2019S), lin-15(+)]	(Cooper et al. 2015)
DJM050	age-1(hx546) II; cwrIs856 [Pdat-1::GFP, Pdat-1::LRRK2(G2019S), lin-15(+)]	
JVR321	nuo-6(qm200); cwrIs856 [Pdat-1::GFP, Pdat-1::LRRK2(G2019S), lin-15(+)])	
DJM049	glp-1(e2141); cwrIs856 [Pdat-1::GFP, Pdat-1::LRRK2(G2019S), lin-15(+)]	

Strain	Genotype	Original publication
JVR320	eat-2(ad1116) II.; cwrIs856 [Pdat-1::GFP, Pdat-1::LRRK2(G2019S), lin-15(+)])	
JVR315	ife-2(ok306) X.; cwrIs856 [Pdat-1::GFP, Pdat-1::LRRK2(G2019S), lin-15(+)])	
DJM048	osm-5(ok451); cwrIs856 [Pdat-1::GFP, Pdat-1::LRRK2(G2019S), lin-15(+)]	
DJM068	rsks-1(ok1255) III; cwrIs856 [Pdat-1:: GFP, Pdat-1::LRRK2(G2019S), lin-15(+)]	
DJM067	daf-16(mu86) I; age-1(hx546) II; cwrIs856 [Pdat-1::GFP, Pdat-1::LRRK2 (G2019S), lin-15(+)]	
DJM063	age-1(hx546) II; cwrIs856 [Pdat-1::GFP, Pdat-1::LRRK2(G2019S), lin-15(+)] ; wpdEx7 (pUnc-119::AGE1Orf::letutr + pMyo-3::RFP)	
DJM064	age-1(hx546) II; cwrIs856 [Pdat-1::GFP, Pdat-1::LRRK2(G2019S), lin-15(+)]; wpdEx8 (pUnc-119::AGE1Orf::letutr + pMyo-3::RFP)	
DJM065	age-1(hx546) II; cwrIs856 [Pdat-1::GFP, Pdat-1::LRRK2(G2019S), lin-15(+)]; wpdEx9 (pDat-1::AGE1Orf::let858 + pMyo-3::RFP)	
DJM066	age-1(hx546) II; cwrIs856 [Pdat-1::GFP, Pdat-1::LRRK2(G2019S), lin-15(+)]; wpdEx10 (pDat-1::AGE1Orf::let858 + pMyo-3::RFP)	
TU3401	sid-1(pk3321) V; uIs69[pCFJ90(myo-2p:: mCherry) + unc-119p::sid-1] V	(Calixto et al. 2010)
DJM001	[Pdat-1::GFP, lin-15(+)]; sid-1(pk3321) V; uIs69[pCFJ90(myo-2p::mCherry) + unc-119p::sid-1] V	
DJM002	[Pdat-1::GFP, Pdat-1::LRRK2(G2019S), lin-15(+)]; sid-1(pk3321) V; uIs69 [pCFJ90(myo-2p::mCherry) + unc-119p:: sid-1] V	

3. Results

3.1. G2019S LRRK2 induces age-dependent dopaminergic neuronal damage but does not influence lifespan

This study seeks to explore the role of different age-related pathways in regulating pathogenic phenotypes in a G2019S LRRK2 worm model of PD. We have employed a transgenic model expressing full-length human G2019S LRRK2 under the control of the presynaptic dopamine transporter promoter (Dat-1). A pDat-1::GFP transgene expressed in *cis* serves as a method to visualize the eight dopaminergic neurons in *C. elegans* from a total of ~302 neurons. Previous studies have demonstrated that this model shows reduced dopaminergic neuronal function as indicated by subtle movement phenotypes and age-related changes in dopaminergic neurons monitored using pDat-1::GFP (Cooper et al. 2015; Yao et al. 2010). The pDat-1::LRRK2(G2019S); pDat-1::GFP line (cwrIs856) is hereafter referred to as LRRK2(G2019S). Similar transgenic lines comprised of integrated arrays marked by pDat-1::GFP together with human wild-type (WT) LRRK2 [cwrIs722] or the PD-linked mutant LRRK2(R1441C) [cwrIs851], and an integrated pDat-1::GFP line (cwrIs730) alone lacking human LRRK2, serve as controls.

Our study focuses primarily on age-dependent neurodegenerative changes within the four anterior cephalic dopaminergic neurons (CEPs), as these neurons are relatively large in size with extended axonal processes and are simple to distinguish from intestinal autofluorescence (lipofuscin accumulation). Our initial validation of this model reveals that CEP neurons expressing LRRK2(G2019S) or LRRK2(R1441C) remain morphologically

normal and indistinguishable from pDat-1::GFP and LRRK2(WT) controls through adult day 6 (Fig. 1A). By adult day 9, GFP-positive puncta are observed within and proximal to the CEP neuronal soma of both mutant LRRK2 transgenics. By day 12, GFP-positive puncta are observed throughout the axon and dendrites in mutant LRRK2 transgenic worms, and GFP intensity within processes is reduced. Changes in cell soma morphology (i.e. swelling, reduced circularity) are also observed. As organismal aging continues to day 15, axonal processes become increasingly disorganized, and GFP intensity in the cell soma is greatly reduced. In LRRK2(G2019S) or LRRK2(R1441C) dopaminergic neurons, GFP appears to coalesce in puncta within the axon, as these remain bright despite the loss of GFP within the cell soma and dendritic processes. The GFP-positive puncta are consistent with the formation of axonal spheroids or inclusions that are commonly observed in degenerating neurons. At advanced ages (days 12–15), dopaminergic expression of pDat-1::GFP is markedly reduced in both pDat-1::GFP and pDat-1::GFP; LRRK2(WT) lines, however, GFP-positive puncta are not observed, demonstrating that this phenotype is specific to PD-linked mutants of LRRK2.

Based on these observations, we developed a robust scoring metric graded from 0 (normal) to 5 (maximum damage) to quantify overall damage in the four CEP dopaminergic neurons that incorporates measures of relative intensity of GFP, the formation of GFP-positive puncta in cell soma and processes, abnormal cell soma morphology (swelling, reduced circularity) and the disorganization of neuronal processes (Fig. 1B). To further validate this scoring metric, worms expressing pDat-1::GFP alone or together with LRRK2(WT), LRRK2(G2019S) or LRRK2(R1441C) were assessed at days 6, 9, 12 and 15, revealing that expression of PD-linked LRRK2 mutants induces pronounced dopaminergic neuronal damage at early time points with the accumulation of damage in an age-dependent manner compared to GFP alone (Fig. 1C). A modest reduction in GFP intensity and increased axonal disorganization are observed during aging in pDat-1::GFP and pDat-1::GFP; pDat-1:: LRRK2(WT) control lines compared to LRRK2(G2019S) or LRRK2 (R1441C) lines. Despite the robust dopaminergic neuronal damage induced by LRRK2(G2019S) or LRRK2(R1441C) expression, we observe that survival and mean lifespan in these strains is not significantly altered compared to pDat-1::GFP control (Fig. 1D–E and S1) and wild-type N2 worms (Fig. 2 and S1), as observed previously (Cooper et al. 2015; Yao et al. 2010). Together, our data describe a worm model of PD whereby expression of PD-linked mutant LRRK2 induces robust age-dependent dopaminergic neuronal damage while lifespan remains unaffected.

3.2.   Lifespan extension of LRRK2(G2019S) worms by genetic reduction of multiple negative regulators of longevity

To determine whether LRRK2-mediated neurodegeneration is impacted by alternative modes of lifespan extension, the LRRK2 (G2019S) model was crossed to a well-characterized panel of genetic mutants known to extend lifespan (negative regulators of longevity, Table 1), including: *daf-2*, the insulin/IGF-1 receptor (Kenyon et al. 1993; Kimura et al. 1997); *age-1* (PI3K) (Friedman and Johnson 1988), a downstream effector kinase in the insulin/IGF-1 signaling pathway; *nuo-6*, a mitochondrial complex I subunit (Yang and Hekimi 2010); *glp-1* (NotchR), required for germline proliferation (Arantes-Oliveira et al.

2002); *eat-2*, a genetic model of caloric restriction (Lakowski and Hekimi 1998); *rsks-1* (S6K), a downstream effector kinase of TOR signaling to regulate protein synthesis (Hansen et al. 2007; Pan et al. 2007); *ife-2* (eIF4E), a translation initiation factor (Hansen et al. 2007), and *osm-5*, an intraflagellar transport protein mediating chemosensation (Apfeld and Kenyon 1999). Initially, we sought to confirm that lifespan would be extended in all mutant backgrounds. On a wild-type background, the pDat-1::GFP; pDat-1::LRRK2(G2019S) transgenic worms exhibit a normal lifespan at 20 °C similar to control pDat-1::GFP or wild-type N2 worms (Figs. 1, 2 and S1) (Cooper et al. 2015; Yao et al. 2010). When crossed into lifespan-extending mutant backgrounds, the mean lifespan of LRRK2(G2019S) worms is increased to a similar extent compared to each genetic mutant alone (Fig. 2 and Table 1). Genetic mutants suppressing insulin/IGF-1 signaling (*daf-2* [*e1370*] and *age-1* [*hx546*]) have the strongest effect on lifespan extension, increasing mean lifespan to 39.1 days and 33.4 days of adulthood, respectively (Fig. 2I and Table 1). Lifespan is extended to a mean of 29.6 days in a *glp-1* mutant lacking germ cells, while mitochondrial respiration (*nuo-6*), TOR signaling (*rsks-1*), caloric intake (*eat-2*), and eIF4E-mediated protein translation (*ife-2*) mutants extend normal lifespan by ~9 days over LRRK2(G2019S) alone or a wild-type N2 strain (Fig. 2I and Table 1). Reduction of chemosensory perception (*osm-5*) results in a more modest ~20% increase in lifespan relative to control worms (Fig. 2I and Table 1). Overall, these data demonstrate that lifespan can be successfully extended using a diverse panel of genetic mutants in LRRK2 (G2019S) transgenic worms similar to non-transgenic control worms.

3.3. Lifespan-extending pathways provide neuroprotection against dopaminergic neuronal damage in LRRK2(G2019S) worms

We next assessed the extent to which different longevity pathways interact with LRRK2(G2019S)-induced neurotoxicity by monitoring damage to GFP-positive dopaminergic CEP neurons, comparing LRRK2 (G2019S) transgenic worms on a wild-type background to lifespan-extending mutant backgrounds under identical conditions. Using the scoring metric validated in Fig. 1, dopaminergic neuronal damage was assessed at day 14 of adulthood, a timepoint where degeneration is clearly observed but neurons largely remain intact. Intriguingly, we find that all pathways of lifespan extension confer variable neuroprotection in the LRRK2(G2019S) model with reduced dopaminergic neuronal damage scores (Fig. 3). In each of the eight lifespan-extending paradigms evaluated, CEP neuronal soma and axonal processes appear visibly healthier and brighter, with wider continuous processes that have increased GFP intensity and reduced GFP-positive puncta (Fig. 3A). However, GFP-positive puncta are still detected in each mutant background, albeit at reduced levels, perhaps suggesting that mechanisms directly mediating LRRK2-induced toxicity are only partly impacted, and that overall organismal health is maintained for an extended period. Interestingly, we note that the degree of neuroprotection afforded by each mutant does not directly correlate with the degree of lifespan extension (Figs. 2I and 3B). Linear regression analysis confirms the general trend that the extent of lifespan extension negatively correlates with degree of dopaminergic damage, as best exemplified by the opposing effects of *daf-2* and *osm-5* (Fig. 3C). Certain lifespan-extending mutants, however, reveal that dopaminergic neuroprotection can be uncoupled from lifespan extension, resulting in an R^2 value of 0.427. For example, *nuo-6* displays a moderate increase in

lifespan yet shows pronounced reduction of dopaminergic damage, and likewise *age-1* shows robust lifespan extension yet a corresponding smaller degree of neuroprotection (Fig. 3C). Collectively, these data demonstrate that delaying aging via multiple distinct pathways is broadly neuroprotective against G2019S LRRK2-induced neurotoxicity, yet lifespan extension does not strictly correlate with the magnitude of neuroprotection. Our data suggest that age-related pathways may functionally interact with G2019S LRRK2-dependent pathways to differing extents, specifically insulin signaling (*daf-2*), mitochondrial respiration (*nuo-6*) and TOR signaling (*rsks-1*), to mediate robust neuroprotection.

It is possible that lifespan-extending mutant backgrounds could provide neuroprotection against G2019S LRRK2 by down-regulating human LRRK2 transgene expression driven by the pDat-1 promoter. To address this possibility, quantitative RT-PCR was performed in a subset of lifespan-extending mutant lines expressing LRRK2(G2019S), compared with the LRRK2(G2019S) strain on a wild-type background. At day 10 of adulthood, we find that human LRRK2 or eGFP mRNA expression levels are not significantly reduced in lifespan-extending mutant backgrounds compared to LRRK2(G2019S) alone (Fig. S2). We observe instead that LRRK2 and GFP transcripts are significantly increased in the *daf-2* background compared to other strains, perhaps reflecting a biologically younger transcriptome. Our data confirm that neuroprotection observed in lifespan-extending mutants does not result from the transcriptional down-regulation of LRRK2 via reduced activity of the Dat-1 promoter.

3.4. Neuroprotective effects of age-1 in the LRRK2(G2019S) model require DAF-16/FOXO

Neuronal health of LRRK2(G2019S)-expressing dopaminergic neurons is preserved in both the *daf-2* and *age-1* lifespan-extending backgrounds. AGE-1/PI3K functions as a downstream effector of the insulin receptor DAF-2 to control nuclear localization of the master transcriptional regulator DAF-16/FOXO. DAF-16/FOXO functions as a downstream factor required for a number of lifespan-regulating pathways, including nutrient and stress-related pathways (Insulin/IGF-1, TOR, caloric restriction, AMPK, JNK) as well as germline signaling. Accordingly, the ability of *daf-2* and *age-1* mutants to increase lifespan are dependent on DAF-16 (Tissenbaum 2018). We previously demonstrated that the protective effects of *daf-2* in LRRK2(G2019S) worms were dependent on the presence of DAF-16 (Cooper et al. 2015). We confirm that lifespan extension and dopaminergic neuroprotection in LRRK2 (G2019S) worms conferred by *age-1*(*hx546*) similarly requires DAF-16 function by crossing *age-1*;LRRK2(G2019S) worms into a *daf-16* (*mu86*) mutant background. The introduction of *daf-16* effectively and fully reverses the increased lifespan (Fig. 4A, B) and dopaminergic protective effects (Fig. 4C) mediated by *age-1*. As the rate of aging is increased in worms with a *daf-16* mutation, dopaminergic damage was scored at day 10 as opposed to day 14. These data demonstrate that *age-1* and *daf-2* similarly require the canonical insulin/IGF-1 signaling pathway functioning upstream of DAF-16/FOXO for mediating neuroprotection in LRRK2(G2019S) transgenic worms.

3.5. Reduced longevity increases dopaminergic neuronal damage in LRRK2(G2019S) worms

While the disruption of genes negatively regulating longevity results in lifespan extension (i.e. *daf-2*), certain genes can also be manipulated to oppositely reduce lifespan. To further

understand the relationship between lifespan and neuroprotection, we employed genetic mutants known to reduce lifespan to explore the impact on dopaminergic neuronal damage. Worms expressing the LRRK2(G2019S) transgene were crossed into strains carrying mutations in the global transcriptional regulator FOXO (*daf-16 [mu86]*) or the α-subunit of AMP-activated protein kinase AMPK (*aak-2 [ok524]*). These two factors mediate growth, metabolism, and stress response pathways, and reducing their activity results in shortened lifespan (Apfeld et al. 2004; Kenyon et al. 1993). Lifespan is robustly reduced in LRRK2(G2019S) worms on a *daf-16* or *aak-2* mutant background, compared to a wild-type background (Fig. 5A, B). However, we observe that the mean lifespan of *daf-16* and *aak-2* mutants carrying the LRRK2(G2019S) transgene is modestly increased relative to *daf-16* and *aak-2* mutants alone lacking transgenic LRRK2 (Fig. 5B), similar to our observations in lifespan-extending mutants (Fig. 2I). Dopaminergic neuronal damage was assessed in these lines at days 9 and 12, time points prior to the mean lifespan of LRRK2 (G2019S) transgenic worms in longevity-reducing backgrounds (*daf-16*: 14.7 ± 0.2 days; *aak-2*: 13.9 ± 0.15 days). At both time points, LRRK2 (G2019S)-induced dopaminergic damage is significantly increased in *daf-16* or *aak-2* backgrounds compared to LRRK2(G2019S) worms on a wild-type background (Fig. 5C, D). These data demonstrate that down-regulation of regulatory pathways associated with *daf-16*/FOXO and *aak-2*/AMPK reduce the lifespan of LRRK2(G2019S) worms while increasing dopaminergic damage at different time points, opposite to the effects of lifespan-extending pathways (Figs. 2–3). While it is possible that the FOXO and AMPK pathways normally function to inhibit LRRK2 signaling or activity, it is also possible the observed increase in dopaminergic neuronal damage may result from systemic changes occurring during accelerated aging. Together, our data further support the observation that lifespan and dopaminergic neuroprotection in LRRK2 (G2019S) worms are positively correlated and functionally interact.

3.6.   Lifespan-extending pathways mediate neuroprotection against G2019S LRRK2 in part via cell-autonomous effects in neurons

LRRK2(G2019S) is specifically expressed in dopaminergic neurons under the control of the Dat-1 promoter with damage limited to these neurons. The aging process requires the coordination of inputs from various tissues including the intestine, neurons and germline; input signaling can be perceived by one tissue but must be relayed to and acted upon by distal tissues. It is unclear whether lifespan-extending pathways mediate dopaminergic neuroprotection in LRRK2(G2019S) worms via their direct actions within neurons themselves, or indirectly, via signals derived from peripheral tissues and organs. To address this question, we performed tissue-specific RNAi-mediated silencing of key lifespan-extending genes to compare the neuronal-specific versus body-wide effects of these pathways on lifespan-extension and neuroprotection against LRRK2(G2019S). We employed an RNAi targeting system using a dsRNA uptake channel SID-1 mutant (Systemic RNAi Deficient, *sid-1* [*qt9*]) combined with a rescuing SID-1 transgene driven by the pan-neuronal Unc-119 promoter (Calixto et al. 2010). In this system, neurons expressing the SID-1 transgene are selectively sensitized to RNAi versus non-neuronal cells that lack SID-1. Body-wide or systemic RNAi in a wild-type background has limited impact on gene expression in neurons as prior studies have suggested that *C. elegans* neurons are largely resistant to RNAi (Asikainen et al. 2005; Kamath et al. 2001; Timmons et al. 2001). The

pDat-1::LRRK2(G2019S); pDat-1::GFP transgene was crossed into the neuronal-sensitizing pUnc-119::SID-1; *sid-1(qt9)* background, referred to hereafter as LRRK2(G2019S); SID-1. Relative to the wild-type background expressing LRRK2(G2019S) line capable of experiencing body-wide RNAi, the neuronal-specific RNAi LRRK2(G2019S); SID-1 line has a reduced mean lifespan when grown on control RNAi (empty vector) (Fig. 6A–B), suggesting that depletion of RNAi machinery within multiple cell types and tissues has a modest impact on longevity.

Bacterial feeding clones from the Ahringer RNAi knockout library targeting lifespan-regulating pathways were verified by sequencing and first confirmed for lifespan extension phenotypes under systemic knockdown conditions prior to studies comparing systemic and neuron-specific RNAi. Clones for *eat-2* and *osm-5* were not available in the RNAi library. Instead, clones targeting related members of the chemoperception pathway (*che-3* and *osm-6*) were tested, but neither extended lifespan following RNAi-mediated knockdown and were not tested further (Fig. S3). We find that the LRRK2(G2019S) [systemic RNAi] and LRRK2(G2019S); SID-1 [neuron-specific RNAi] backgrounds both exhibit marked lifespan extension in response to RNAi targeting the insulin/IGF-1 pathway (*daf-2*, *age-1*) (Figs. 6A–B and S4, Table 2). Surprisingly, neuron-specific RNAi to *age-1* results in a 1.46-fold increase in lifespan similar to systemic RNAi (1.35-fold), suggesting that the lifespan-regulating functions of AGE-1/PI3K are mediated primarily via the neuronal population. Interestingly, RNAi for *daf-2* demonstrates a stronger increase in lifespan with systemic (1.23-fold) compared to neuronal (1.16-fold) knockdown. These data are in agreement with previous studies demonstrating that pan-neuronal restoration of insulin/IGF-1 function partially rescues extended lifespan in mutant backgrounds (Iser and Wolkow 2007; Wolkow et al. 2000). Importantly, the dopaminergic degenerative phenotype in LRRK2(G2019S) worms is suppressed by systemic or neuronal RNAi for *age-1* and *daf-2* (Fig. 6C–D), similar to data obtained with genetic mutants (Fig. 3), thereby suggesting that the insulin/IGF-1 signaling pathway can interact with aging and neurodegeneration via both cell autonomous and non-cell autonomous functions.

Similar to the insulin/IGF-1 pathway, targeting *rsks-1* by systemic or neuronal-specific RNAi induces lifespan extension (Fig. 6A–B and S4, Table 2), suggesting longevity-regulating functions can occur in both neuronal and non-neuronal tissues. The pan-neuronal or systemic reduction of *rsks-1* function reduces dopaminergic neuronal damage in LRRK2(G2019S) worms to a similar extent (Fig. 6C–D), although TOR pathway signaling has a greater impact on lifespan in peripheral tissues (1.2-fold) versus neurons (1.1-fold) (Table 2). Systemic RNAi for *nuo-6* results in early larval arrest and embryonic lethality (Fig. 6A and S4), as observed previously (Fraser et al. 2000; Rual et al. 2004; Sonnichsen et al. 2005; Yang and Hekimi 2010), that precludes further analysis. However, neuronal-specific RNAi for *nuo-6* results in modest lifespan extension (Fig. 6B and S4) yet a marked reduction in dopaminergic neuronal damage (Fig. 6D) in LRRK2(G2019S) worms. These data suggest a direct role for mitochondrial respiration in LRRK2(G2019S)-induced dopaminergic phenotypes that can be uncoupled from mechanisms associated with lifespan extension induced by mitochondrial dysfunction. In contrast, systemic or neuronal-specific knockdown of *ife-2* induces marked lifespan extension (Fig. 6A–B and S4, Table 2) but fails to protect against G2019S LRRK2-induced dopaminergic damage (Fig. 6C–D),

demonstrating that neuroprotection does not strictly correlate with extended longevity. Collectively, our data suggest that age-related pathways can directly function in part within neurons (*age-1*, *daf-2*, *nuo-6*, *rsks-1*) to mediate lifespan extension and dopaminergic neuroprotection in LRRK2(G2019S) worms.

3.7. Restoration of AGE-1/PI3K in neurons differentially modulates lifespan and dopaminergic neuronal damage in LRRK2(G2019S); age-1 worms

Using tissue-specific RNAi, we demonstrate that a number of lifespan-regulating pathways mediate systemic effects on longevity via signaling occurring within neuronal populations, as well as exerting lifespan-regulating effects in peripheral non-neuronal tissues and cells. It is possible that reduced LRRK2(G2019S)-induced dopaminergic damage observed in lifespan-extending conditions can be attributed to systemic pathways regulating organismal aging, as both insulin/IGF-1 signaling and mitochondrial dysfunction can function via non-cell-autonomous mechanisms (Apfeld and Kenyon 1998; Iser and Wolkow 2007; Libina et al. 2003; Wolkow et al. 2000; Zhang et al. 2013). Alternatively, signaling could be required within specific cells or populations to directly regulate their viability and health. To address whether insulin/IGF-1 signaling functions specifically within dopaminergic neurons to impact LRRK2(G2019S)-induced neurotoxicity, we compared the extent of neuroprotection in LRRK2(G2019S); *age-1* worms with restoration of AGE-1 specifically targeted to dopaminergic neurons or pan-neuronally. We generated extrachromosomal transgenic arrays that drive expression of AGE-1/PI3K cDNA under the control of the pan-neuronal Unc-119 promoter or the dopaminergic-specific Dat-1 promoter, that were crossed into long-lived LRRK2(G2019S); *age-1* (*hx546*) worms for rescue studies. We elected to focus on the AGE-1/PI3K pathway for these studies since RNAi targeting of *age-1* in neurons produces robust effects on both lifespan and neuroprotection compared to other pathways suggesting a prominent role in neurons (Fig. 6). In these new lines, lifespan and dopaminergic neuronal damage were monitored.

Pan-neuronal (pUnc-119-driven) expression of AGE-1 is able to rescue lifespan extension conferred by *age-1*(*hx546*), while dopaminergic-specific AGE-1 restoration does not impact longevity (Fig. 7A–B). These data demonstrate that AGE-1 function is required in neurons in general to regulate lifespan, as previously suggested (Iser and Wolkow 2007; Wolkow et al. 2000), whereas AGE-1 in dopaminergic neurons does not participate in lifespan. At day 14, dopaminergic neuronal damage in LRRK2(G2019S) worms is pronounced (score = 4.1 ± 0.06), and the introduction of *age-1* rescues neuronal damage (score = 2.81 ± 0.06) (Fig. 7C–D). Restoration of AGE-1 expression in dopaminergic neurons (pDat-1::AGE-1) is sufficient to significantly and partially restore neuronal damage induced by LRRK2(G2019S) (score = 3.28 ± 0.07) (Fig. 7C–D). These data suggest that interactions between AGE-1 and LRRK2(G2019S) can occur cell-autonomously within dopaminergic neurons, despite also having a non-cell-autonomous role in lifespan regulation. Surprisingly, pan-neuronal restoration of AGE-1 further enhances protection (reduces damage) in dopaminergic neurons (score = 2.34 ± 0.08) beyond the protective effects of *age-1* alone (Fig. 7C–D). Similar results with respect to lifespan extension and dopaminergic neuronal damage are observed with at least two independent array lines expressing AGE-1 (Fig. S5). These complex data suggest that dopaminergic neuronal health may be regulated directly by

cell-autonomous AGE-1 signaling, as well as indirectly by non-cell-autonomous inputs arising from outside the nervous system. The observation that expressing AGE-1 in neurons of LRRK2(G2019S); *age-1* worms decreases lifespan but increases neuronal survival demonstrates that lifespan and neuroprotection can be experimentally dissociated.

4. Discussion

Understanding LRRK2 pathophysiological mechanisms is critical for defining cellular pathways and targets that are amenable to therapeutic intervention for attenuating neurodegeneration in *LRRK2*-linked PD. In this study, we evaluate how distinct mechanisms regulating the aging process interact with human LRRK2(G2019S)-induced dopaminergic neurodegeneration, addressing whether longevity is intrinsically coupled to dopaminergic neuronal health. We first demonstrate that mean lifespan of LRRK2(G2019S) worms can be successfully extended by different age-related pathways, including reduction of insulin/IGF-1 signaling (*daf-2*; *age-1*), TOR signaling (*rsks-1*), caloric intake (*eat-2*), chemoperception (*osm-5*), germline function (*glp-1*) or mitochondrial function (*nuo-6*). Next, we compared how LRRK2(G2019S)-induced dopaminergic degeneration was impacted by genetic mutants with different levels of lifespan extension. We find that age-dependent neuronal damage induced by LRRK2(G2019S) is broadly regulated by distinct lifespan-extending pathways, with extended longevity generally correlating with dopaminergic neuroprotection. Importantly, our data demonstrate that neuroprotection against LRRK2(G2019S) is not simply limited or specific to *daf-2*, as we previously reported (Cooper et al. 2015), but extends beyond insulin-IGF-1 signaling. However, we find that lifespan-extending paradigms variably influence the extent of neuroprotection with a non-linear relationship between lifespan and dopaminergic damage in the LRRK2(G2019S) model. These data suggest that lifespan extension per se is not sufficient alone for protection, and supports instead a specific interaction between certain age-related pathways and LRRK2(G2019S)-related pathogenic mechanisms, including most prominently insulin/IGF-1 signaling, TOR-mediated protein translation, and mitochondrial respiration. Our study highlights these age-related pathways as important for *LRRK2*-linked disease that now warrant further mechanistic studies in mammalian LRRK2 models.

The tissue specificity mediating the interaction between LRRK2 (G2019S) and lifespan-regulating factors was examined using neuronal-specific versus body-wide (non-neuronal) RNAi-mediated gene silencing. Neuronal-specific or body-wide knockdown of *age-1*, *daf-2*, *rsks-1*, and *nuo-6* are sufficient to induce lifespan extension and reduce LRRK2(G2019S)-induced dopaminergic damage, suggesting roles for these pathways in both neuronal and peripheral non-neuronal cells. However, one clear example of lifespan extension being experimentally dissociated from neuroprotection is provided by *ife-2* knockdown that extends lifespan with body-wide or neuronal-specific RNAi yet fails to impact dopaminergic degeneration. Interestingly, we find that mitochondrial dysfunction-induced lifespan extension via *nuo-6* depletion interacts with LRRK2(G2019S) both in a systemic genetic mutant and with neuronal-specific RNAi, leading to a modest increase in lifespan yet a dramatic reduction of LRRK2(G2019S)-induced neurotoxicity. *Nuo-6* therefore provides another example of this dissociation that may imply this mitochondrial-related pathway rather than lifespan extension most likely drives the protective interaction with

LRRK2(G2019S). The loss of *nuo-6* function, and impaired mitochondrial complex-I activity, appears to contradict long-held observations that mitochondrial impairment contributes to PD (Singh et al. 2019). It is important to note that *nuo-6* genetic mutation or body-wide RNAi both induce early lethality in worms, but not when limited to neurons, implying that the beneficial effects of lowering *nuo-6* arise solely from neurons. Mitochondrial dysfunction is sensed and adapted to early in *C. elegans* development (Dillin et al. 2002), leading to upregulation of stress response and other related pathways that may specifically protect against LRRK2(G2019S) later in life. It is most likely therefore that these stress-related adaptations in neurons rather than complex-I deficits induced by reduced *nuo-6* levels are sufficient to mediate neuroprotection.

Our study also focused on the insulin/IGF-1 signaling pathway as a mechanism of delayed aging and increased neuroprotection in the LRRK2(G2019S) model of PD. Reducing insulin receptor signaling or increasing DAF-16/FOXO activity specifically in adipose or neuroendocrine tissue has been shown to increase lifespan in worms, flies and mice (Apfeld and Fontana 2017), and has been shown to have both cell-autonomous and non-cell-autonomous roles in the regulation of lifespan and other metabolic processes. In agreement with previous studies (Iser and Wolkow 2007; Pan et al. 2011; Tank et al. 2011; Toth et al. 2012; Wolkow et al. 2000), we find that the insulin/IGF-1 signaling pathway is involved in nervous system aging, including preservation of dopaminergic neuronal integrity and survival. We find that specifically restoring AGE-1/PI3K function in dopaminergic neurons is sufficient to partially reverse the neuroprotective effects against LRRK2(G2019S) mediated by *age-1* disruption. However, pan-neuronal restoration of AGE-1 activity, which is capable of reversing lifespan extension in systemic *age-1* mutants, appears to have an opposite effect on dopaminergic neurodegeneration induced by LRRK2(G2019S). This unexpected finding demonstrates that the insulin/IGF-1 signaling pathway likely acts in both a cell-autonomous (i.e. dopaminergic) and non-cell-autonomous manner with respect to neuronal health, perhaps through the activation of stress response pathways in non-dopaminergic neurons and/or peripheral tissues that elicit further neuroprotection against LRRK2(G2019S). This observation highlights the importance of studying neurodegeneration and potential therapeutic interventions in the context of the whole organism.

Advanced age is the most significant determinant of clinical prognosis for PD patients and impacts the severity of motor and non-motor symptoms as well as the efficacy of common treatments, including levodopa (Collier et al. 2017). While diagnosis with the disease is thought not to impact human life expectancy, comorbid cognitive impairments and related complications can negatively affect patient outcomes (Savica et al. 2017). It remains unclear how dysfunction of specific age-related pathways predispose some individuals to develop this common neurodegenerative disease, while others can harbor mutations in PD-linked genes and avoid clinical symptoms. Given the difficulty of working with human samples, due in part to variability in environmental influences and genetic background, seminal studies defining the well-conserved longevity-regulating pathways examined in this study have been performed in non-human model organisms, thus, the applicability of these findings to human lifespan and disease remains to be established. However, the lifespan determining pathways first defined in invertebrate models, including the insulin/IGF-1 axis,

TOR and AMPK signaling, and ETC dysfunction have proven relevant in mice and non-human primates, demonstrating conservation of lifespan-regulating genetic pathways across evolutionary distance, and suggesting that at least a subset of longevity-regulating dynamics are applicable to human aging and disease. Indeed, pharmacological studies with FDA-approved drugs including the TOR inhibitor rapamycin and metformin, which inhibits ETC Complex-I function and increases AMPK levels, have been shown to extend lifespan in several species and may prevent or alleviate multiple chronic diseases in humans (Campisi et al. 2019). Broad spectrum improvements in healthspan may result from targeting the intersecting and complex molecular pathways regulating aging, and may thus provide potential therapeutic opportunities for PD patients. However, questions remain as to whether specific age-related mechanisms could be manipulated to successfully prevent disease. Our findings pertaining to *nuo-6* are particularly interesting as genes in the electron transport chain are similarly down-regulated in aged worms, flies, mice and humans (Zahn et al. 2006), and given that dopaminergic neurons may be specifically sensitive to oxidative damage due to high levels of dopamine metabolism, it is possible that interventions specifically targeting mitochondrial respiration may be most beneficial in treating PD.

5. Conclusions

Our study provides insight into the pathogenesis of *LRRK2*-linked PD and longevity regulation. We find that LRRK2(G2019S)-induced neurodegeneration is strongly influenced by distinct pathways governing the overall rate of aging and lifespan, including insulin/IGF-1 signaling, the TOR pathway, and mitochondrial respiration. These and other lifespan-regulating pathways are highly conserved and associate with major signaling pathways. While distinct sets of factors are engaged downstream, mechanisms of lifespan modulation at least partially overlap, and cross-talk between signaling pathways may partly account for the observed complexity. LRRK2 has been shown to interact with different cell signaling pathways, specifically those involved in protein degradation, mitochondrial and endolysosomal functions. Further examination of the interplay between these pathways may reveal common factors influencing LRRK2-dependent neurotoxicity, and future studies will require validation of these mechanisms in genetic rodent models of PD. Overall, our study highlights that systemic aging of the organism and neuronal degeneration are related phenomena, but in a non-linear manner, and suggests that insulin/IGF-1 signaling is compartmentalized within different cells and tissues of an organism that are potentially differentially regulated during aging. Taken together, our study highlights specific lifespan-regulating pathways that may provide a number of promising therapeutic targets for inhibiting LRRK2-dependent neurodegeneration in PD.

Supplementary Material

Refer to Web version on PubMed Central for supplementary material.

Acknowledgments

References

Apfeld J, Fontana W, 2017. Age-dependence and aging-dependence: neuronal loss and lifespan in a *C. elegans* model of Parkinson's disease. Biology (Basel) 7.

Apfeld J, Kenyon C, 1998. Cell nonautonomy of *C. elegans* daf-2 function in the regulation of diapause and life span. Cell 95, 199–210. [PubMed: 9790527]

Apfeld J, Kenyon C, 1999. Regulation of lifespan by sensory perception in *Caenorhabditis elegans*. Nature 402, 804–809. [PubMed: 10617200]

Apfeld J, et al., 2004. The AMP-activated protein kinase AAK-2 links energy levels and insulin-like signals to lifespan in *C. elegans*. Genes Dev. 18, 3004–3009. [PubMed: 15574588]

Arantes-Oliveira N, et al., 2002. Regulation of life-span by germ-line stem cells in *Caenorhabditis elegans*. Science 295, 502–505. [PubMed: 11799246]

Asikainen S, et al., 2005. Selective sensitivity of *Caenorhabditis elegans* neurons to RNA interference. Neuroreport 16, 1995–1999. [PubMed: 16317341]

Billingsley KJ, et al., 2018. Genetic risk factors in Parkinson's disease. Cell Tissue Res. 373, 9–20. [PubMed: 29536161]

Brenner S, 1974. The genetics of *Caenorhabditis elegans*. Genetics. 77, 71–94. [PubMed: 4366476]

Calixto A, et al., 2010. Enhanced neuronal RNAi in *C. elegans* using SID-1. Nat. Methods 7, 554–559. [PubMed: 20512143]

Campisi J, et al., 2019. From discoveries in ageing research to therapeutics for healthy ageing. Nature 571, 183–192. [PubMed: 31292558]

Collaborators GBDN, 2019. Global, regional, and national burden of neurological disorders, 1990–2016: a systematic analysis for the Global Burden of Disease Study 2016. Lancet Neurol. 18, 459–480. [PubMed: 30879893]

Collier TJ, et al., 2017. Aging and Parkinson's disease: different sides of the same coin? Mov. Disord 32, 983–990. [PubMed: 28520211]

Cooper JF, et al., 2015. Delaying aging is neuroprotective in Parkinson's disease: a genetic analysis in *C. elegans* models. NPJ Parkinsons Dis. 1, 15022. [PubMed: 28725688]

Di Maio R, et al., 2018. LRRK2 activation in idiopathic Parkinson's disease. Sci. Transl. Med 10.

Dillin A, et al., 2002. Rates of behavior and aging specified by mitochondrial function during development. Science 298, 2398–2401. [PubMed: 12471266]

Dorsey ER, et al., 2018. The emerging evidence of the Parkinson pandemic. J. Parkinsons Dis 8, S3–S8. [PubMed: 30584159]

Erb ML, Moore DJ, 2020. LRRK2 and the endolysosomal system in Parkinson's disease. J. Parkinsons Dis 10, 1271–1291. [PubMed: 33044192]

Fraser AG, et al., 2000. Functional genomic analysis of *C. elegans* chromosome I by systematic RNA interference. Nature 408, 325–330. [PubMed: 11099033]

Friedman DB, Johnson TE, 1988. A mutation in the age-1 gene in *Caenorhabditis elegans* lengthens life and reduces hermaphrodite fertility. Genetics 118, 75–86. [PubMed: 8608934]

Hansen M, et al., 2007. Lifespan extension by conditions that inhibit translation in *Caenorhabditis elegans*. Aging Cell 6, 95–110. [PubMed: 17266679]

Hernandez DG, et al., 2016. Genetics in Parkinson disease: Mendelian versus non-Mendelian inheritance. J. Neurochem 139 (Suppl. 1), 59–74. [PubMed: 27090875]

Ho PW, et al., 2020. Age-dependent accumulation of oligomeric SNCA/alpha-synuclein from impaired degradation in mutant LRRK2 knockin mouse model of Parkinson disease: role for therapeutic

activation of chaperone-mediated autophagy (CMA). Autophagy 16, 347–370. [PubMed: 30983487]

Iser WB, Wolkow CA, 2007. DAF-2/insulin-like signaling in *C. elegans* modifies effects of dietary restriction and nutrient stress on aging, stress and growth. PLoS One 2, e1240. [PubMed: 18043747]

Islam MS, Moore DJ, 2017. Mechanisms of LRRK2-dependent neurodegeneration: role of enzymatic activity and protein aggregation. Biochem. Soc. Trans 45, 163–172. [PubMed: 28202670]

Kamath RS, et al., 2001. Effectiveness of specific RNA-mediated interference through ingested double-stranded RNA in *Caenorhabditis elegans*. Genome Biol. 2. RESEARCH0002.

Kenyon C, et al., 1993. A *C. elegans* mutant that lives twice as long as wild type. Nature 366, 461–464. [PubMed: 8247153]

Kimura KD, et al., 1997. Daf-2, an insulin receptor-like gene that regulates longevity and diapause in *Caenorhabditis elegans*. Science 277, 942–946. [PubMed: 9252323]

Kluss JH, et al., 2019. LRRK2 links genetic and sporadic Parkinson's disease. Biochem. Soc. Trans 47, 651–661. [PubMed: 30837320]

Lakowski B, Hekimi S, 1998. The genetics of caloric restriction in *Caenorhabditis elegans*. Proc. Natl. Acad. Sci. U. S. A 95, 13091–13096. [PubMed: 9789046]

de Lau LM, Breteler MM, 2006. Epidemiology of Parkinson's disease. Lancet Neurol. 5, 525–535. [PubMed: 16713924]

Libina N, et al., 2003. Tissue-specific activities of *C. elegans* DAF-16 in the regulation of lifespan. Cell. 115, 489–502. [PubMed: 14622602]

Longo F, et al., 2017. Age-dependent dopamine transporter dysfunction and Serine129 phospho-alpha-synuclein overload in G2019S LRRK2 mice. Acta Neuropathol. Commun. 5, 22.

Marder K, et al., 2015. Age-specific penetrance of LRRK2 G2019S in the Michael J. Fox Ashkenazi Jewish LRRK2 Consortium. Neurology 85, 89–95. [PubMed: 26062626]

Mir R, et al., 2018. The Parkinson's disease VPS35[D620N] mutation enhances LRRK2-mediated Rab protein phosphorylation in mouse and human. Biochem. J 475, 1861–1883. [PubMed: 29743203]

Nass R, et al., 2002. Neurotoxin-induced degeneration of dopamine neurons in *Caenorhabditis elegans*. Proc. Natl. Acad. Sci. U. S. A 99, 3264–3269. [PubMed: 11867711]

Pan KZ, et al., 2007. Inhibition of mRNA translation extends lifespan in *Caenorhabditis elegans*. Aging Cell 6, 111–119. [PubMed: 17266680]

Pan CL, et al., 2011. Genetic analysis of age-dependent defects of the *Caenorhabditis elegans* touch receptor neurons. Proc. Natl. Acad. Sci. U. S. A 108, 9274–9279. [PubMed: 21571636]

Priess JR, et al., 1987. The glp-1 locus and cellular interactions in early *C. elegans* embryos. Cell 51, 601–611. [PubMed: 3677169]

Ramonet D, et al., 2011. Dopaminergic neuronal loss, reduced neurite complexity and autophagic abnormalities in transgenic mice expressing G2019S mutant LRRK2. PLoS One 6, e18568. [PubMed: 21494637]

Rual JF, et al., 2004. Toward improving *Caenorhabditis elegans* phenome mapping with an ORFeome-based RNAi library. Genome Res. 14, 2162–2168. [PubMed: 15489339]

Savica R, et al., 2017. Survival and causes of death among people with clinically diagnosed synucleinopathies with parkinsonism: a population-based study. JAMA Neurol. 74, 839–846. [PubMed: 28505261]

Singh A, et al., 2019. LRRK2 and mitochondria: recent advances and current views. Brain Res. 1702, 96–104. [PubMed: 29894679]

Sonnichsen B, et al., 2005. Full-genome RNAi profiling of early embryogenesis in *Caenorhabditis elegans*. Nature. 434, 462–469. [PubMed: 15791247]

Spatola M, Wider C, 2014. Genetics of Parkinson's disease: the yield. Parkinsonism Relat. Disord 20 (Suppl. 1), S35–S38. [PubMed: 24262184]

Steger M, et al., 2016. Phosphoproteomics reveals that Parkinson's disease kinase LRRK2 regulates a subset of Rab GTPases. Elife 5.

Syntichaki P, et al., 2007. eIF4E function in somatic cells modulates ageing in *Caenorhabditis elegans*. Nature 445, 922–926. [PubMed: 17277769]

Tank EM, et al., 2011. Spontaneous age-related neurite branching in *Caenorhabditis elegans*. J. Neurosci 31, 9279–9288. [PubMed: 21697377]

Timmons L, et al., 2001. Ingestion of bacterially expressed dsRNAs can produce specific and potent genetic interference in *Caenorhabditis elegans*. Gene. 263, 103–112. [PubMed: 11223248]

Tissenbaum HA, 2018. DAF-16: FOXO in the context of *C. elegans*. Curr. Top. Dev. Biol 127, 1–21. [PubMed: 29433733]

Toth ML, et al., 2012. Neurite sprouting and synapse deterioration in the aging *Caenorhabditis elegans* nervous system. J. Neurosci 32, 8778–8790. [PubMed: 22745480]

Van Raamsdonk JM, Hekimi S, 2011. FUdR causes a twofold increase in the lifespan of the mitochondrial mutant gas-1. Mech. Ageing Dev 132, 519–521. [PubMed: 21893079]

West AB, et al., 2005. Parkinson's disease-associated mutations in leucine-rich repeat kinase 2 augment kinase activity. Proc. Natl. Acad. Sci. U. S. A 102, 16842–16847. [PubMed: 16269541]

Wolkow CA, et al., 2000. Regulation of *C. elegans* life-span by insulinlike signaling in the nervous system. Science. 290, 147–150. [PubMed: 11021802]

Xiong Y, et al., 2018. Robust kinase- and age-dependent dopaminergic and norepinephrine neurodegeneration in LRRK2 G2019S transgenic mice. Proc. Natl. Acad. Sci. U. S. A 115, 1635–1640. [PubMed: 29386392]

Yang W, Hekimi S, 2010. Two modes of mitochondrial dysfunction lead independently to lifespan extension in *Caenorhabditis elegans*. Aging Cell 9, 433–447. [PubMed: 20346072]

Yao C, et al., 2010. LRRK2-mediated neurodegeneration and dysfunction of dopaminergic neurons in a *Caenorhabditis elegans* model of Parkinson's disease. Neurobiol. Dis 40, 73–81. [PubMed: 20382224]

Zahn JM, et al., 2006. Transcriptional profiling of aging in human muscle reveals a common aging signature. PLoS Genet. 2, e115. [PubMed: 16789832]

Zhang P, et al., 2013. Direct and indirect gene regulation by a life-extending FOXO protein in *C. elegans*: roles for GATA factors and lipid gene regulators. Cell Metab. 17, 85–100. [PubMed: 23312285]
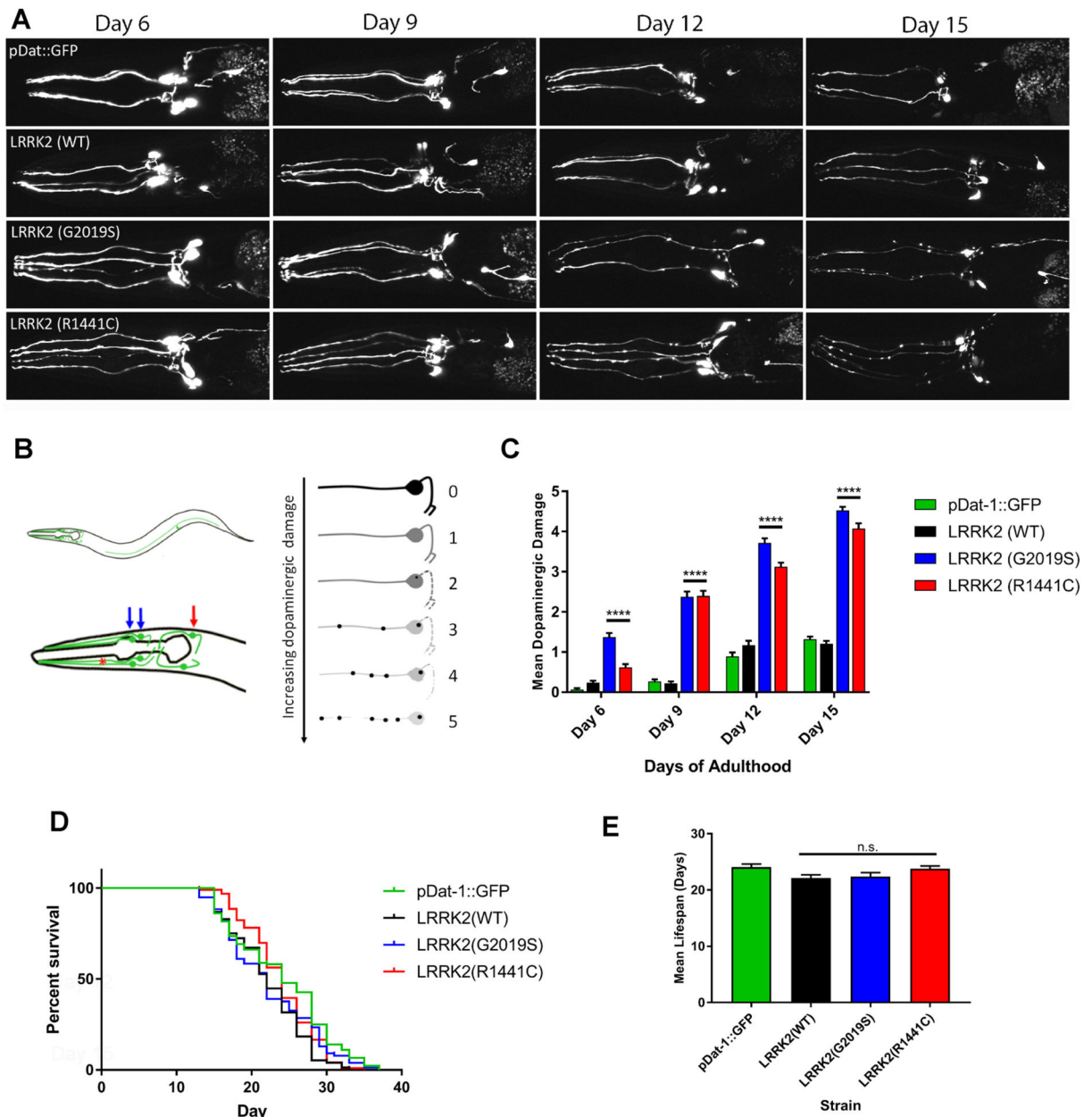
Fig. 1.

Human LRRK2(G2019S) expression in worms induces age-dependent dopaminergic neuronal damage without altering lifespan. A) Dopaminergic neurons are marked by GFP driven by the dopamine transporter (Dat-1) promoter. pDat-1::GFP and pDat-1::GFP; pDat-1::hLRRK2(WT) worms serve as control lines compared to pDat-1-driven transgenic lines expressing common PD-linked LRRK2 mutations (R1441C and G2019S) in addition to pDat-1::GFP. Representative maximum projection confocal micrographs depict dopaminergic neurons on days 6, 9, 12 and 15. In controls strains, GFP intensity is reduced with aging, while LRRK2 mutations (R1441C and G2019S) induce accumulation of GFP-positive puncta associated with increased degeneration. Images are oriented with the mouth to the left. B) *C. elegans* dopaminergic signaling is carried out by 8 neurons from a total of

302 neurons. Two pairs of cephalic neurons (CEP, blue arrows) are the most anterior, followed by the anterior deirids (ADE, red arrows) located proximal to the nerve ring, and the laterally positioned posterior deirid pair (PDE). The axonal processes of the CEP neurons (red asterisk) extend toward the anterior, while the branched neuritic processes project distally into the synapse-rich nerve ring. The 0–5 scoring metric accounts for the overall morphology and damage of individual CEP dopaminergic cell soma and neurites, the presence and localization of GFP-positive dense puncta (internal versus external to cell body), and overall GFP intensity within individual neurons. C) Graph comparing dopaminergic neuronal damage to CEP neurons in worms expressing GFP alone, LRRK2(WT), or PD-linked LRRK2 mutations (R1441C and G2019S) at days 6, 9, 12 and 15. Data represent dopaminergic damage with scoring from 0 to 5 (mean ± SEM; n = 78–181 CEP neurons/group across 3 independent experiments). LRRK2-expressing transgenics were compared to pDat-1::GFP control worms at each timepoint by one-way ANOVA with Dunnett's post-test (****P< 0.0001, as indicated). Significant and progressive neuronal damage scores are induced by PD-linked LRRK2 mutations relative to WT LRRK2 or GFP alone. D) Kaplan-Meier survival analysis comparing pDat-1::GFP control (green) and lines expressing pDat-1::GFP together with LRRK2(WT) (black), LRRK2(G2019S) (blue), and LRRK2(R1441C) (red). LRRK2 transgenic lines display a normal lifespan compared to pDat-1::GFP expressed in a wild-type background as indicated by mean longevity (E, mean ± SEM, n = 76–136 animals/group across 3 experiments). One-way ANOVA finds no significant differences between mean lifespan of pDat-1::GFP (cwrIs730, green), pDat-1::LRRK2(WT) (cwrIs722, black), pDat-1::LRRK2(G2019S) (cwrIs856, blue) and pDat-1::LRRK2(R1441C) (cwrIs851, red) worms. Specific N used to generate graphs can be found in Tables S1 (lifespan) and S2 (dopaminergic damage).
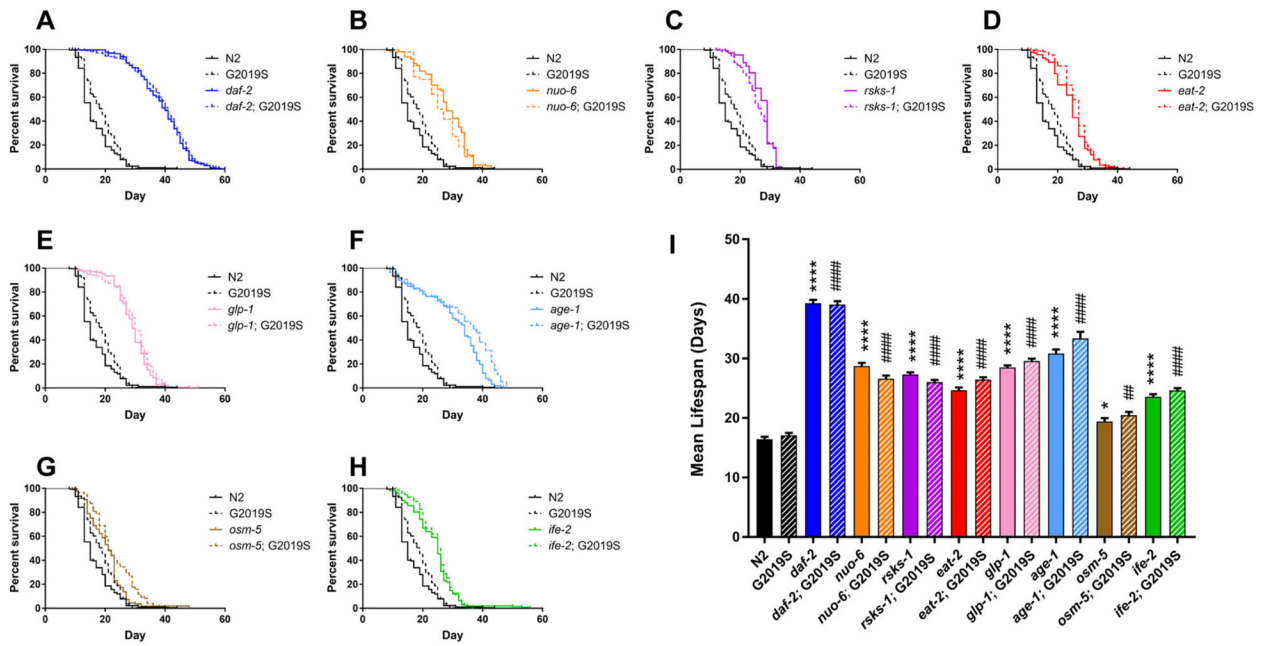
Fig. 2.
Genetic mutation of negative longevity regulators extends the lifespan of LRRK2(G2019S) transgenic worms. A-H) Kaplan-Meier survival curves comparing longevity of wild-type (N2, black solid) and LRRK2(G2019S) (black dashed) worms with lifespan-extending genetic mutants alone (color solid) and LRRK2(G2019S) transgenics on each mutant background (color dashed). Curves represent combined data from at least 3 individual experiments ($n = 96$–292 animals). I) Mean lifespan from data shown in A-H. Bars represent mean ± SEM. *$P < 0.05$ or ****$P < 0.0001$ compared to WT (N2), ##$P < 0.01$ or ####$P < 0.0001$ compared to LRRK2(G2019S), by one-way ANOVA with Bonferroni's multiple comparisons test. Specific N used to generate graphs can be found in Table S3.
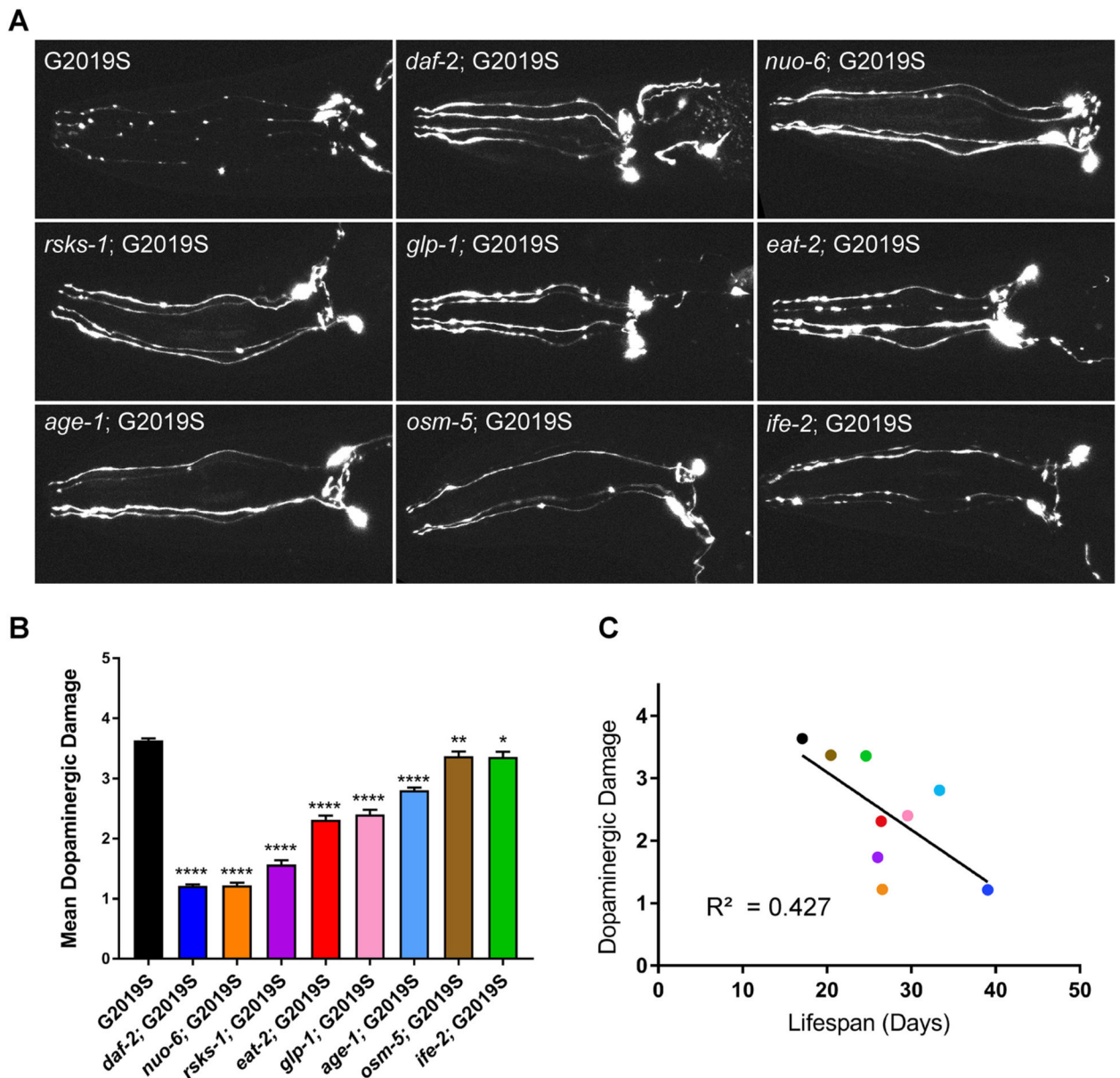
Fig. 3.
Lifespan extension is broadly neuroprotective in the LRRK2(G2019S) worm model. A) Representative maximum projection confocal images of anterior GFP-positive CEP dopaminergic neurons at day 14 of adulthood from LRRK2(G2019S) on a wild-type or genetic mutant background. Images reveal reduced yet variable neuronal damage in all lifespan-extending backgrounds. B) Quantification of CEP dopaminergic neuronal damage at day 14 using the 0–5 scoring metric. Bars represent the mean ± SEM damage from 3 individual experiments (n = 171–2181 CEP neurons/group). *$P < 0.05$, **$P < 0.005$ or ****$P < 0.0001$ compared to LRRK2(G2019S) alone by one-way ANOVA with Dunnett's post-hoc test. C) Linear regression analysis ($R^2 = 0.4266$) of mean lifespan (in days) relative to mean dopaminergic neuronal damage (0–5 score) for each worm strain, reveals a general

inverse correlation indicating that lifespan extension is broadly associated with reduced neuronal damage. Specific *N* used to generate graphs can be found in Table S3.
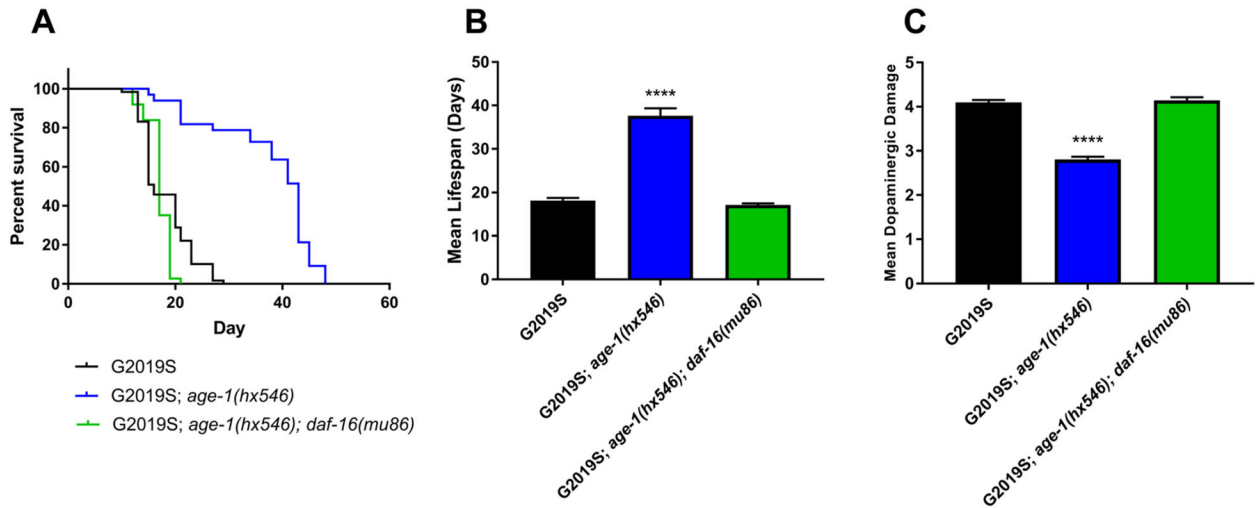
Fig. 4.

Lifespan extension and neuroprotection mediated by *age-1* mutant in LRRK2(G2019S) worms is dependent on DAF-16. Kaplan-Meier survival curve (A) and mean lifespan (B) of LRRK2(G2019S) worms on a wild-type background, and on an *age-1* or *age-1; daf-16* genetic background. The *daf-16* mutant fully reverses the extended lifespan conferred by *age-1*. A) Curves represent combined survival data from at least 3 individual experiments (*n* = 59–87 animals/group), whereas B) bars represent mean ± SEM lifespan. C) Quantitation of CEP dopaminergic neuronal damage at day 14 in LRRK2(G2019S) worms on all three genetic backgrounds. An *age-1* mutant markedly reduces neuronal damage compared to the wild-type background, that is fully restored to normal wild-type levels in an *age-1; daf-16* double mutant. Bars represent the mean ± SEM neuronal damage (*n* = 183–413 CEP neurons/group across 3 independent experiments). ****P < 0.0001 compared to LRRK2 (G2019S) alone by one-way ANOVA with Dunnett's post-hoc analysis. Specific *N* used to generate graphs can be found in Table S4.
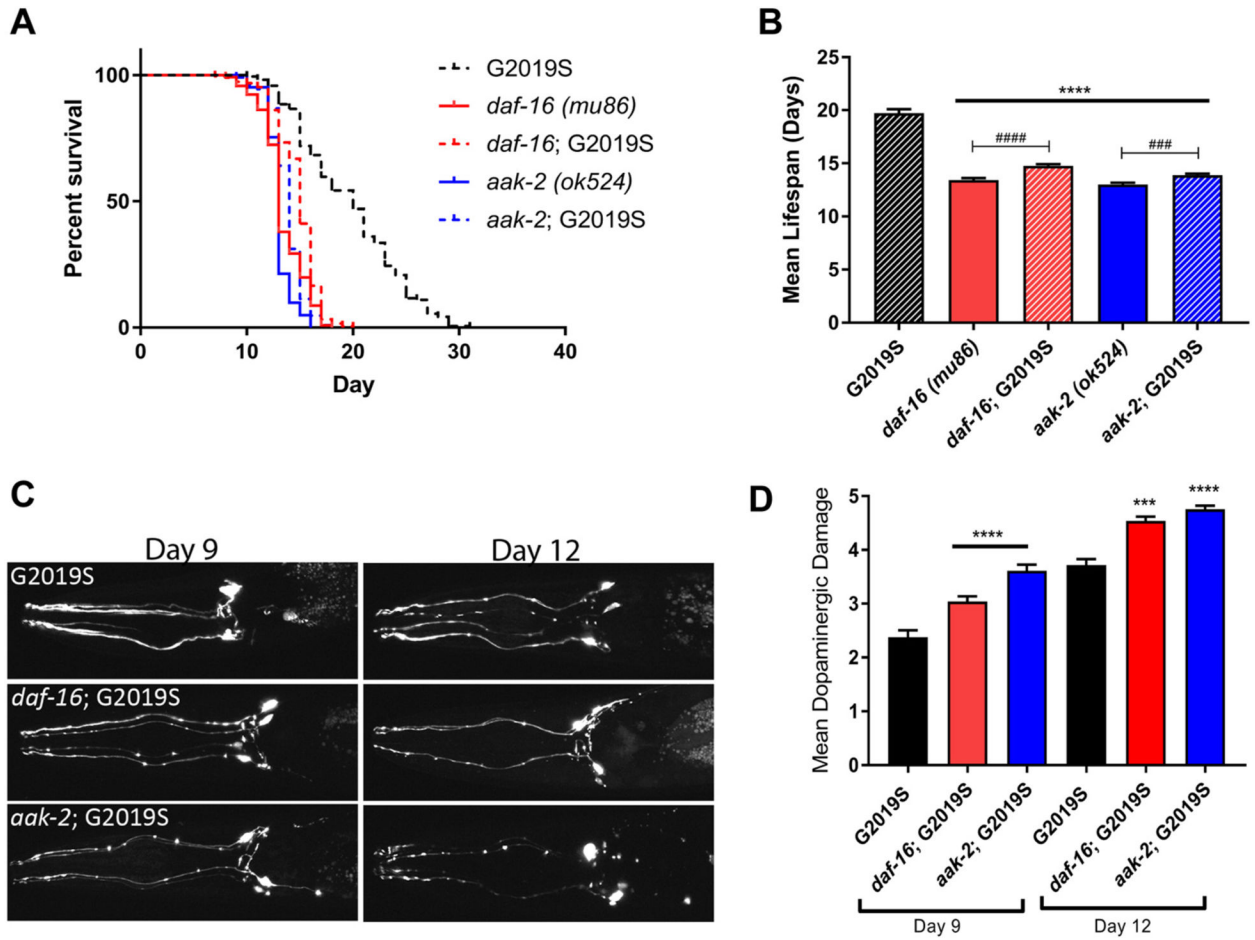
Fig. 5.
Genetic mutation of positive longevity regulators reduces the lifespan of LRRK2(G2019S) worms and enhances neurodegeneration. Kaplan-Meier survival curve (A) and mean lifespan (B) comparing LRRK2(G2019S) on a wild-type background (black dashed) to lifespan-reducing genetic mutants alone (color solid) and LRRK2(G2019S) transgenics on each mutant background (color dashed). Curves/bars represent combined survival data from at least 3 individual experiments ($n = 61–187$ animals/group). Mutation of either *daf-16*/FOXO (red) or *aak-2*/AMPK (blue) significantly reduces the mean lifespan of LRRK2(G2019S) worms, as indicated by one-way ANOVA with Dunnett's post-hoc test (****$P < 0.0001$). LRRK2(G2019S)-expressing worms induce a modest increase in the lifespan of *daf-16* or *aak-2* mutants relative to each mutant alone, yet to a lesser extent than the lifespan of LRRK2(G2019S) alone (###$P < 0.005$ or ####$P < 0.0005$ by two-tailed, unpaired Student's *t*-test, as indicated). As depicted in (C) and quantified in (D), the onset of LRRK2(G2019S)-induced neurodegeneration occurs by an earlier timepoint (day 9–12) and with significantly increased damage scores in lifespan-reducing mutant backgrounds. ***$P < 0.0005$ or ****$P < 0.0001$ by one-way ANOVA with Dunnett's post-hoc test compared to LRRK2(G2019S) alone at each time point. Bars represent the mean ± SEM neuronal damage ($n = 39–151$ CEP neurons/group across 3 independent experiments). Specific *N* used to generate graphs can be found in Tables S5 (lifespan) and S6 (dopaminergic damage).
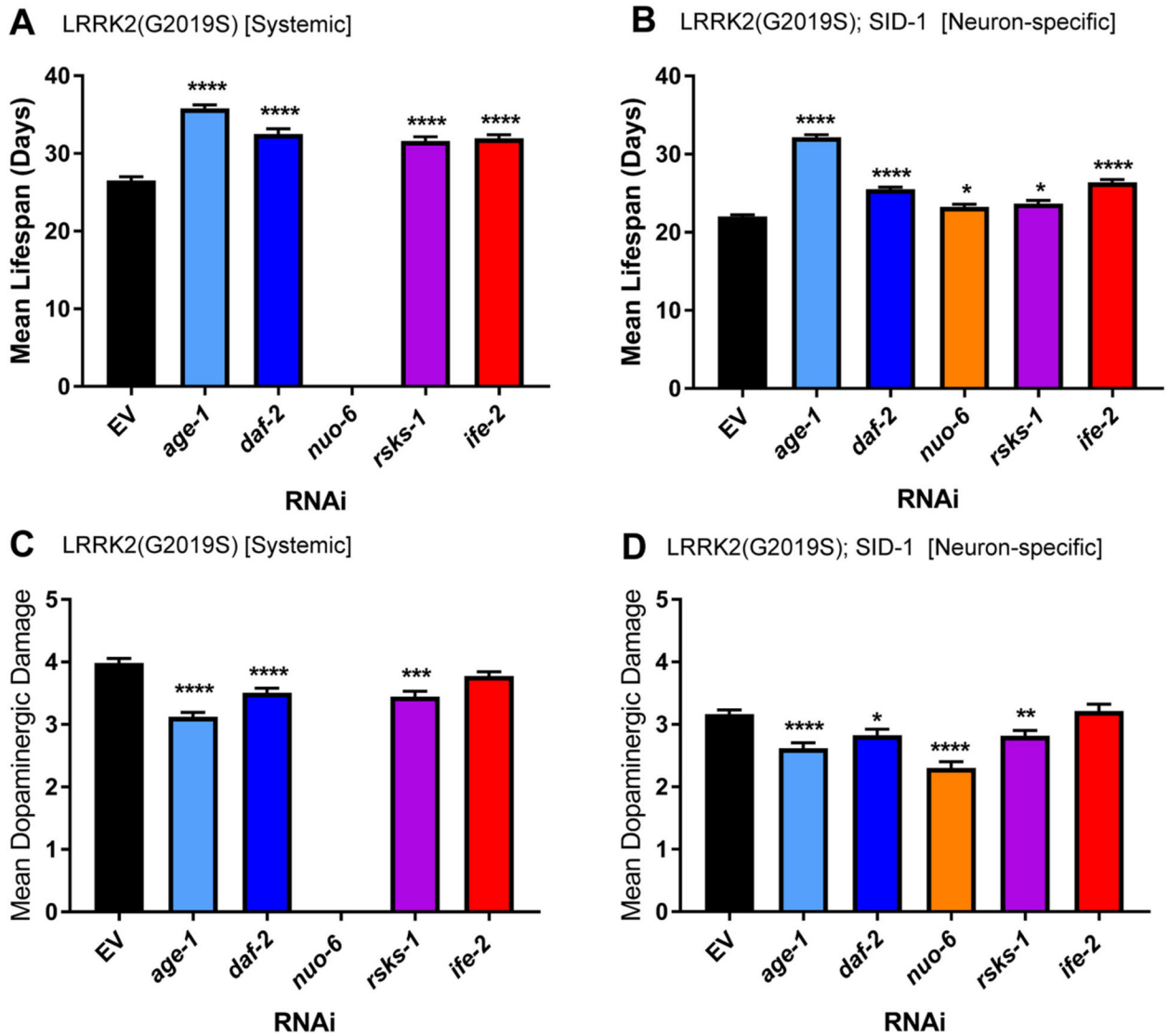
Fig. 6.

Neuronal-specific knockdown of multiple longevity-regulating genes is neuroprotective in the LRRK2(G2019S) worm model. A subset of negative regulators of longevity were targeted by RNAi-mediated knockdown either systemically (body-wide, with reduced efficacy in neurons) (A, C) or specifically within the neuronal cell population using the pUnc-119::SID-1; *sid-1*(pk3321) background (B, D). Mean lifespan of each strain is indicated (A–B). Bars represent the mean ± SEM combined from 3 independent experiments with $n = 111$–278 animals per group. Quantitation of CEP dopaminergic neuronal damage in LRRK2(G2019S) worms with C) systemic body-wide RNAi assessed at day 14, or D) neuronal-specific RNAi assessed at day 11. Note: systemic knockdown of *nuo-6* results in early lethality and cannot be assessed in (A, C). Bars represent the mean ± SEM combined from 3 independent experiments with $n = 221$–764 CEP neurons/group. *$P < 0.05$, **$P < 0.01$, ***$P < 0.001$ or ****$P < 0.0001$ compared to control (empty vector, EV) by one-way ANOVA with Dunnett's post-hoc test. Specific N used to generate graphs can be found in Table S7.
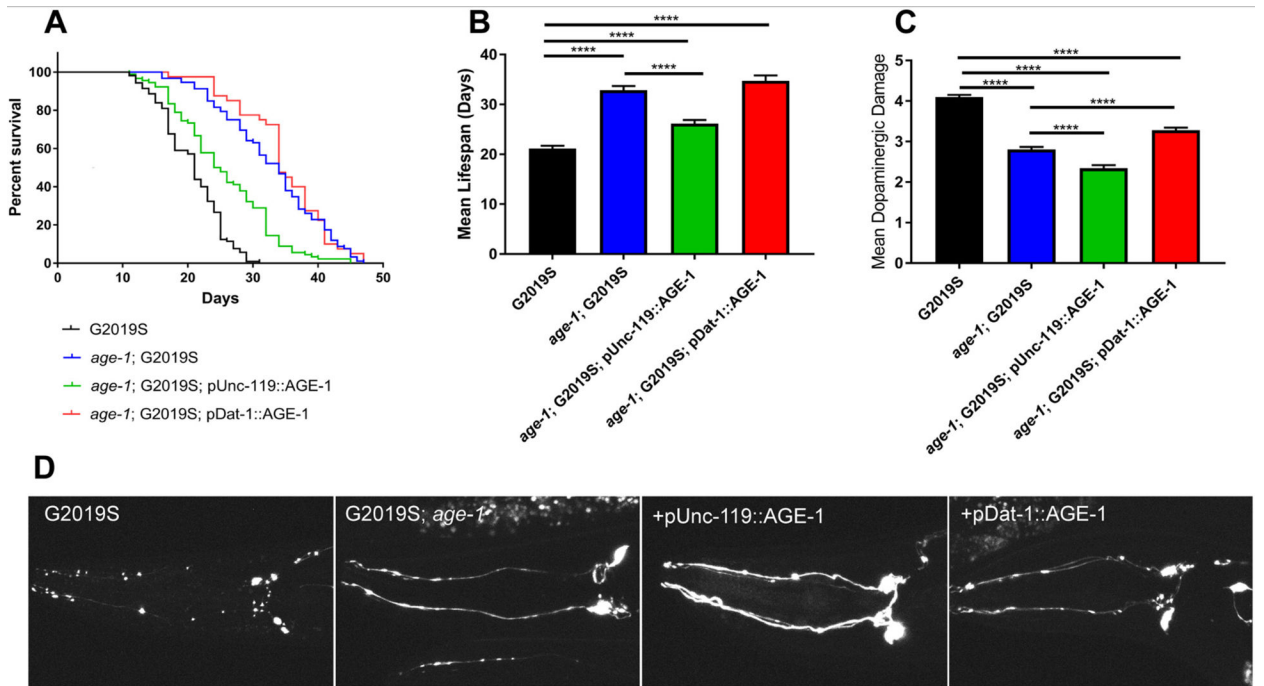
Fig. 7.
Restoring AGE-1/PI3K function in dopaminergic neurons demonstrates a cell-autonomous effect on LRRK2(G2019S)-induced neuronal damage. A) Kaplan-Meier survival curves comparing the lifespan of LRRK2(G2019S) (black), *age-1*; LRRK2(G2019S) (blue), and transgenic lines expressing AGE-1 from pan-neuronal (pUnc-119; green) or dopaminergic-specific (pDat-1; red) promoters in the *age-1*; LRRK2(G2019S) background. B) Mean lifespan of each worm strain from survival data shown (A). Bars represent the mean ± SEM from ≥ 3 independent experiments with $n = 74$–111 animals per group. Extended lifespan in the *age-1* background is partially reverted by pan-neuronal AGE-1 expression. C) Quantification of mean dopaminergic neuronal damage induced by LRRK2(G2019S) at day 14 in wild-type, *age-1* mutant, or in tissue-specific AGE-1 rescue lines on an *age-1* mutant background. Bars represent the mean ± SEM from ≥ 3 independent experiments with $n = 183$–413 CEP neurons/group. ****$P < 0.0001$ between the indicated groups by one-way ANOVA with Dunnett's multiple comparisons post-hoc test. D) Representative maximum projection confocal images of GFP-positive CEP dopaminergic neurons at day 14 in pDat-1::GFP; pDat-1::LRRK2(G2019S) worms on wild-type, *age-1* or transgenic AGE-1 rescue backgrounds. Specific *N* used to generate graphs can be found in Table S8.

Table 1

Comparison of lifespan extension induced by genetic mutants in wild-type and LRRK2(G2019S) worms.

Worm strain	Mean lifespan (days)	Maximum lifespan (days)	Mean lifespan (% of N2 or G2019S)
Wild-type (N2)	16.43	31	-
LRRK2 (G2019S)	**17.08**	**29**	-
daf-2 (e1370)	39.28	60	239.07
***daf-2*; G2019S**	**39.06**	**57**	**228.69**
age-1 (hx546)	30.81	49	187.52
***age-1*; G2019S**	**33.36**	**51**	**195.32**
nuo-6 (qm200)	28.7	43	174.68
***nuo-6*; G2019S**	**26.56**	**44**	**155.50**
rsks-1 (ok1255)	27.3	34	166.16
***rsks-1*; G2019S**	**26.01**	**34**	**152.28**
eat-2 (ad1116)	24.65	36	150.03
***eat-2*; G2019S**	**26.43**	**38**	**154.74**
gp-1 (e2141)	28.48	42	173.34
***gp-1* G2019S**	**29.56**	**44**	**173.07**
ife-2 (ok306)	23.55	35	143.34
***ife-2*; G2019S**	**24.63**	**40**	**144.20**
osm-5 (ok451)	19.42	29	118.20
***osm-5*; G2019S**	**20.46**	**33**	**119.79**

For % mean lifespan, single genetic mutants were compared to N2 worms, whereas double mutants were compared to LRRK2(G2019S) (in bold).

Table 2

Comparison of fold change in lifespan and dopaminergic neuronal damage with systemic or neuronal-specific RNAi knockdown of longevity-regulating genes.

RNAi	Lifespan (fold change versus EV)		Dopaminergic damage (fold change versus EV)	
	Systemic	Neuronal	Systemic	Neuronal
daf-2	1.23	1.16	0.88	0.9
age-1	1.35	1.46	0.78	0.83
rsks-1	1.19	1.08	0.87	0.89
ife-2	1.2	1.2	0.95	1.02
nuo-6	n/a	1.01	n/a	0.73